GENERALISED NONLINEAR MODELING OF UNSTABLE STICK-SLIP FORCE REDUCTION EFFECTS IN FRICTION ENERGY DISSIPATION DEVICES

Geoffrey W Rodgers[1], Oliver Mesnil[2], Jose Chanchi[3], Gregory A. MacRae[3], Charles Clifton[4], and J Geoffrey Chase[1*]

SUMMARY

The Sliding Hinge Joint (SHJ) is an Asymmetric Friction Connection (AFC) developed to create a repeatable, efficient means of dissipating seismic response energy and reducing structural damage without yielding of the structural frame elements. Testing has demonstrated stable efficient hysteretic behaviour. However, it is necessary to fully characterise their dynamic behaviour including any less stable aspects observed in the response of these devices for selected materials. This observed behaviour may reduce device force and energy dissipation, creating an influence on the overall structure that should be fully understood and accounted for in design. This research models the hysteretic behaviour of a SHJ with an zinc anti-corrosion coating that demonstrates less than fully stable experimental dynamic behaviour in contrast to many other SHJ material choices. The model developed uses a stick-slip mechanism based on a variable friction coefficient to capture the observed dynamics with an overall Menegotto-Pinto dynamic hysteretic model. The overall results show how the model may be realistically extended to a more general model that captures observed non-linear dynamics in these and similar friction devices, and yield new insight and design tools for use with these devices.

INTRODUCTION

The Sliding Hinge joint (SHJ) is a device designed to dissipate energy without damage in moment-resisting steel framed structures (MRSFs) designed for seismic resistance (MacRae et al, 2010; Clifton, 2005; Khoo et al, 2012). It is an Asymmetric Friction Connection (AFC) that can undergo large connection rotations with limited or no damage, drastically reducing economic losses due to post-earthquake repair costs and the duration of a building closure after an event, while preventing building collapse and protecting life safety. These outcomes are achieved by bolting the top flange of the beam to the column through the top flange plate, with slotted bolted connections in the beam web and bottom flange of the beam to allow rotation. A typical SHJ is a 5-element friction device placed at the bottom of the connection, as shown in Figure 1.

This type of AFC is an arrangement of five plates, comprising three steel plates and two thinner plates termed shims. The connection is assembled by means of high strength bolts with washers, Belleville washers and nuts. The connection allows relative motion across the shims, which dissipates energy due to the friction exerted by the bolt clamping force across the plates. Figure 2 shows the SHJ specific pieces and Figure 3 the method of action.

Recent research has examined several different shim materials, by experimentally imposing sinusoidal displacement on the moving plate (middle plate) and keeping the left plate fixed (MacRae et al, 2010; Khoo et al,). Most materials exhibit different force levels as a function of shim material and clamping force, due to their specific material properties, but have relatively stable, largely square hysteretic loops. However, some materials, such as Bisalloy 500 with an zinc anti-corrosion coating, can exhibit an inconsistent behaviour, as shown in Figure 4. Such unstable behaviour may degrade the average force and reduce the life of the device, creating unintended variability in the response predicted for design and reducing the overall capacity of a structure to withstand a major seismic event. While the stick-slip behaviour is not necessarily desirable, and other forms of dissipation may be selected which do not exhibit this behaviour for most real structures, the ability to model the behaviour allows overall undesirable effects associated with this behaviour to be quantified.

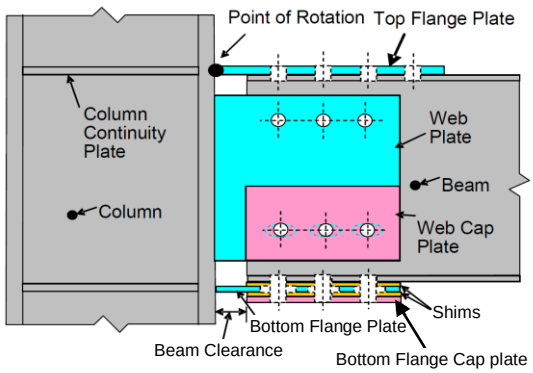

Figure 1: ***Sliding hinge connection schematic showing device and implementation in a steel beam-column connection [1].***

[1] *Department of Mechanical Engineering, University of Canterbury, Christchurch*

[2] *ENSMA, Futuroscope Chasseneuil, France*

[3] *Department of Civil Engineering, University of Canterbury, Christchurch*

[4] *Department of Civil Engineering, University of Auckland.*

* *Corresponding Author: geoff.chase@canterbury.ac.nz*

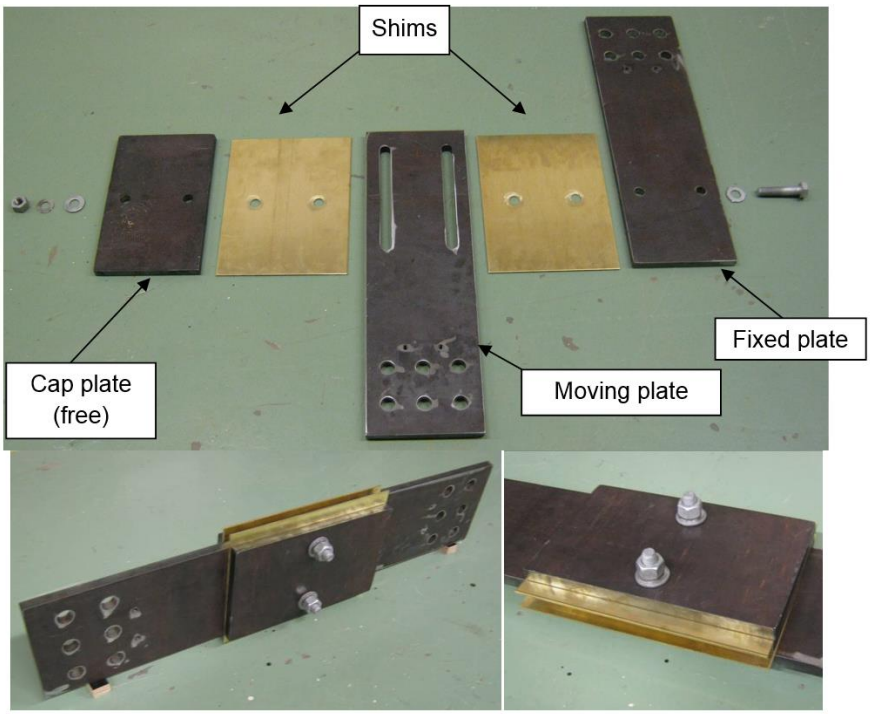

Figure 2: ***SHJ mechanism: Disassembled device (top) and two assembled views***

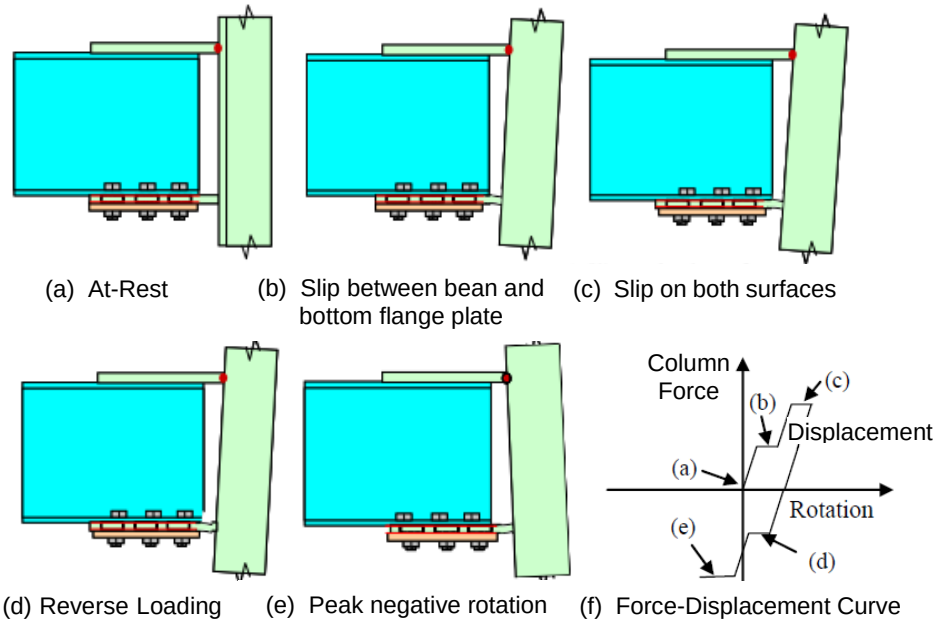

Figure 3: ***Sliding of plates in a SHJ during a cycle at input motion. Friction between the shims and plates dissipates energy resulting in energy dissipation (MacRae et al, 2010).***

This manuscript develops a model to capture this more irregular, stick-slip mechanism to better understand, capture and account for this behaviour.

METHODS

Model 1: Bilinear Menegotto-Pinto and Stick Slip

The Menegotto-Pinto (MP) hysteresis model is used to provide an explicit fundamental mechanics equation for the overall hysteretic loop (Menegotto and Pinto, 1973; Sivaselvan and Reinhorn, 2000). The MP formulation represents a mathematical 'switching' technique whereby a piece-wise linear behaviour can be represented by a continuous mathematical model. The MP equation provides an initial linear stiffness (K) and a constant elastic portion when the force, F_{MP}, exceeds a set value (F_{static}). It is generically defined:

$$F_{MP} = \frac{K.x}{\left(1+\left|\frac{K.x}{F_{static}}\right|^{\beta}\right)^{\frac{1}{\beta}}} \quad (1)$$

where the exponent β defines the transition from the initial linear stiffness to the post-yield behaviour. A higher value ($\beta >> 1$) provides a sharper transition and a lower value ($\beta = 1$ to 5) a much more gradual transition.

When $K.x<F_{static}$, the denominator is equivalent to 1, and the equation is just a standard spring equation following Hooke's law. When $K.x > F_{static}$, the denominator equals $K.x/F_{static}$, such that $F_{MP}=F_{static}$, resulting in bi-linear behaviour. Two further terms are added to 'reset' the MP equation and provide cyclical

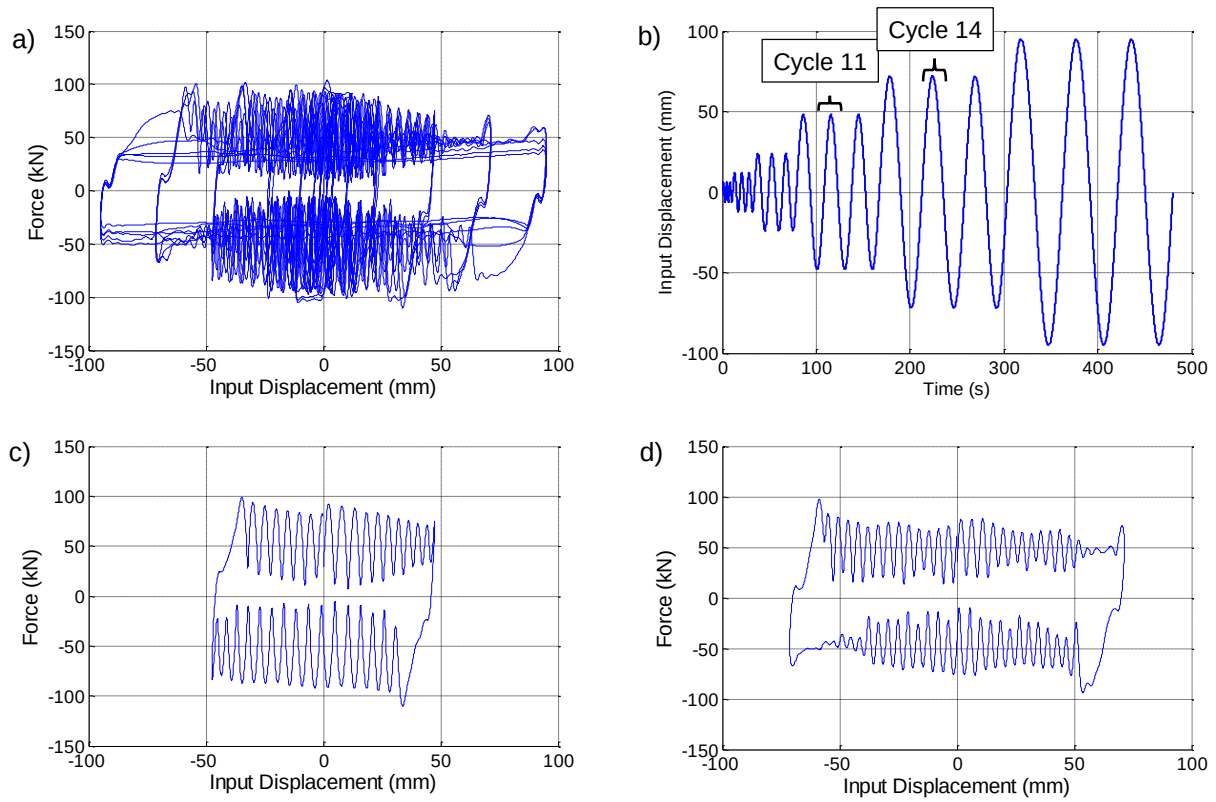

Figure 4: ***Experimental data for zinc coating of Bisalloy 500 material, a) over 18 cycles of increasing magnitude imposed over in 6 steps as shown in b). The data are filtered by a Butterworth filter to remove sensor noise above 1 KHz without losing the underlying mechanics mechanism The bottom two pictures show the 11th c) and the 14th d) cycles individually for clarity to clearly illustrate the stick-slip phenomena.***

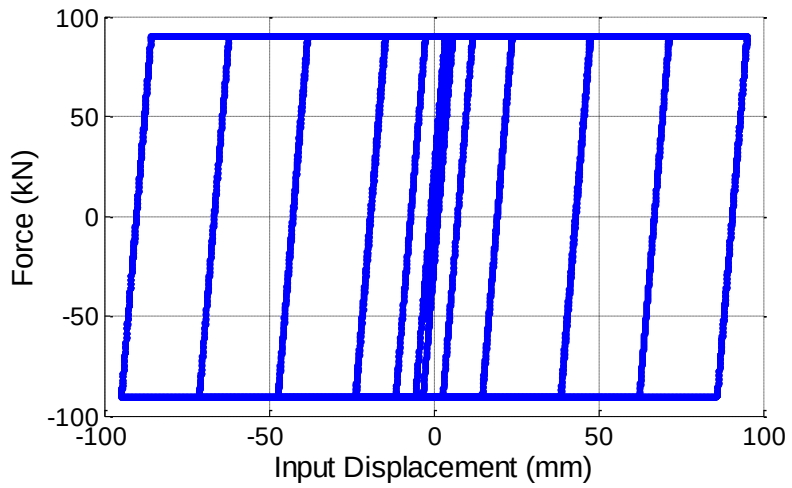

Figure 5: ***Menegotto-Pinto model of Equation 2 using K=20kN/mm, $F_{stastic}$ = 90 kN and β=100.***

behaviour. When the input velocity changes sign, F_{reset} and x_{reset} take the current value of F and x. Therefore, a new effective origin is created at the current position, and the MP equation is referenced back to this reset point. The resulting MP-based model is defined:

$$F_{MP} = \frac{K.(x-x_{reset})+F_{reset}}{\left(1+\left|\frac{K.(x-x_{reset})+F_{reset}}{F_{static}}\right|^{\beta}\right)^{\frac{1}{\beta}}} \qquad (2)$$

A typical result for Equation (2) is shown in the Figure 5, with the same input displacement profile of Figure 4b used in the experiments. It is clear that this model provides a backbone for the results of Figure 4, but does not capture the irregular behaviour.

The irregular oscillations in Figure 4 are hypothesized to be the result of a stick-slip effect. In fact, some wear of the zinc coating is observed experimentally, which can contaminate the friction surfaces and potentially act as a lubricant. As a result, the friction force within the device may vary quite noticably, which should be taken into account in design.

Notably, when such wear debris is evacuated by further motion or manually, the force from the device is observed to increase to expected levels again. Hence, it is hypothesized that this effect is essentially due to dynamic changes in the friction coefficient seen as dynamic changes to F_{static} in Equation (2). In

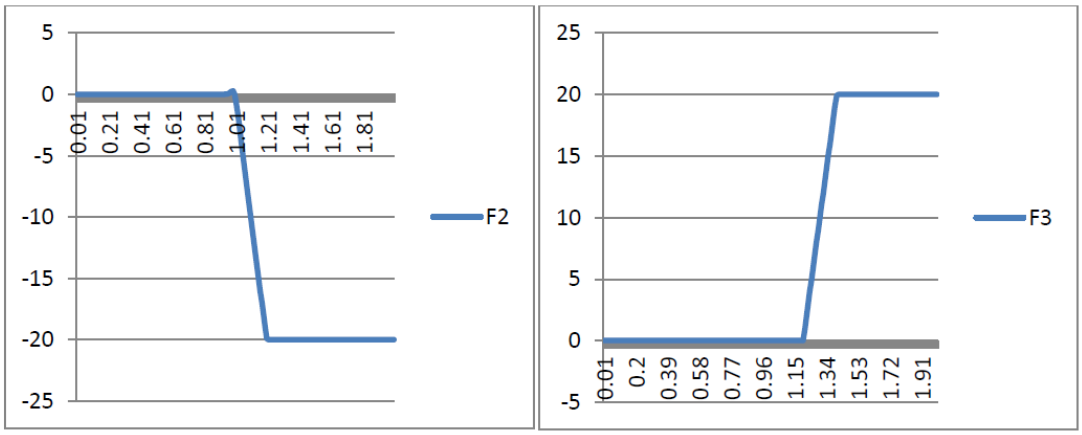

Figure 6: ***Modification to output force for the first half of the first oscillation (left) causing a drop in (positive) force, and the second part of oscillation (right) causing a rise in the (negative) force. Both thus result in reductions in observed device force.***

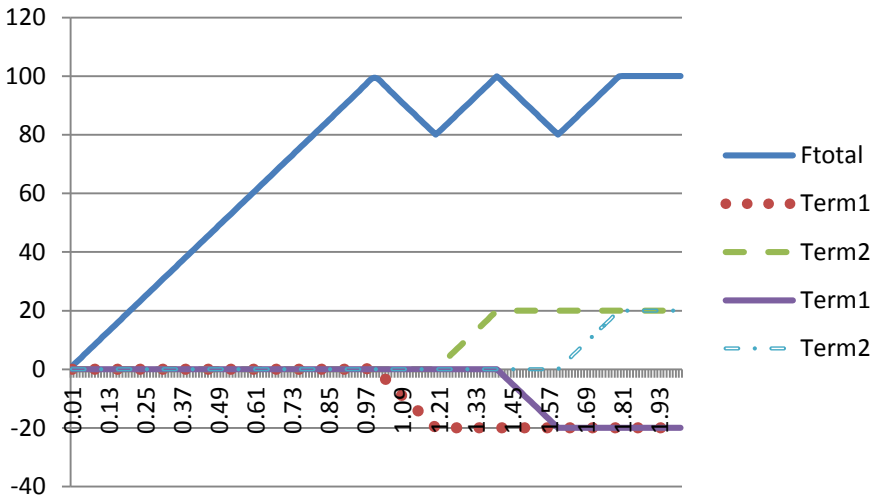

Figure 7: ***MP curve with 2 oscillations having effect of Term1 (F1) and Term2 (F2) to the curve for F_{static} = 100kN, $F_{kinetic}$ =80kN, K=100 kN/mm, $\beta = \gamma$ =100 and Amplitude =F_{static}-$F_{kinetic}$=20kN.***

addition, the amplitude of these oscillations was observed to decrease as displacement continued in a given direction during a cycle, as seen in the bottom panels of Figure 4.

The modelling approach adds local functions to Equation (2) to capture these oscillations as a function of F_{static}. Each oscillation is modelled as a simple linear rise or fall in force resulting from a modification to the behaviour of F_{static} in Equation (2). Figure 6 shows the modifications from the modelled force to capture this stick-slip phenomenon in graphical format.

These terms can be added to Equation (2) as added bi-linear effects, yielding two equations to capture this regime of behaviour, defined:

$$F_2 = \frac{-(K.x - F_{static})}{\left(1+\left|\frac{F_{static}}{K.x}\right|^{\gamma}\right).\left(1+\left|\frac{K.x-F_{static}}{Amplitude}\right|^{\beta}\right)^{1/\beta}} \quad (3)$$

$$F_3 = \frac{K.x+F_{kinetic}-2.F_{static}}{\left(1+\left|\frac{F_{static}}{K.x}\right|^{\gamma}\right).\left(1+\left|\frac{Amplitude}{K.x-F_{Static}}\right|^{\gamma}\right).\left(1+\left|\frac{K.x+F_{kinetic}-2.F_{static}}{Amplitude}\right|^{\beta}\right)^{1/\beta}} \quad (4)$$

Where the denominator has one or two added multiplicative terms.

The first $\left(1+\left|\frac{Amplitude}{K.x-F_{Static}}\right|^{\gamma}\right)$ term provides the first corner of F_2. The second term, defined $\left(1+\left|\frac{K.x+F_{kinetic}-2.F_{static}}{Amplitude}\right|^{\beta}\right)^{1/\beta}$, provides the first corner of F_3 and the second corner of F_2. Figure 7 shows two such cycles once the impact of Terms 1 and 2 are included.

Model 2: Bilinear Menegotto-Pinto with Random Stick Slip Behaviour

The amplitude of oscillations observed in Figure 4 appears effectively random although the average amplitude decreases with increasing input displacement in any one direction. Therefore, if further modelling to capture this behaviour is desired, the amplitude of these changes can be replaced by a random quadratic decreasing function defined by:

$$Amplitude = (F_{static} - F_{kinetic}).\left(1+\frac{rand(0:1)}{2}\right).\left(1-\frac{x^2}{x_{max}{}^2}\right) \quad (5)$$

Where rand(0:1) gives an uniformly distributed random number between 0 and 1, although any random function might be used. Equation (5) allows any observed stick-slip or similar behaviours be captured and generalizes the modelling approach.

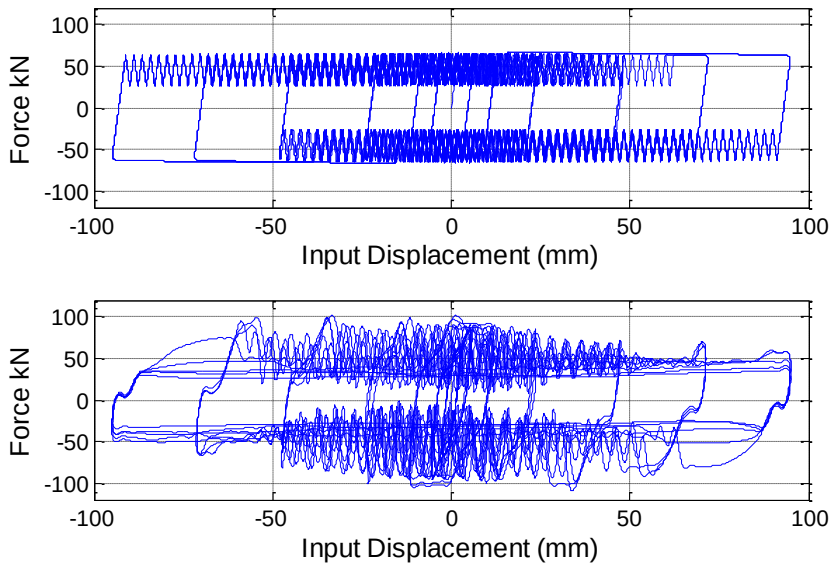

Figure 8: Comparison between Model 1 - Bilinear Menegotto-Pinto with Stick Slip of Equations (3)-(4) - and filtered data.

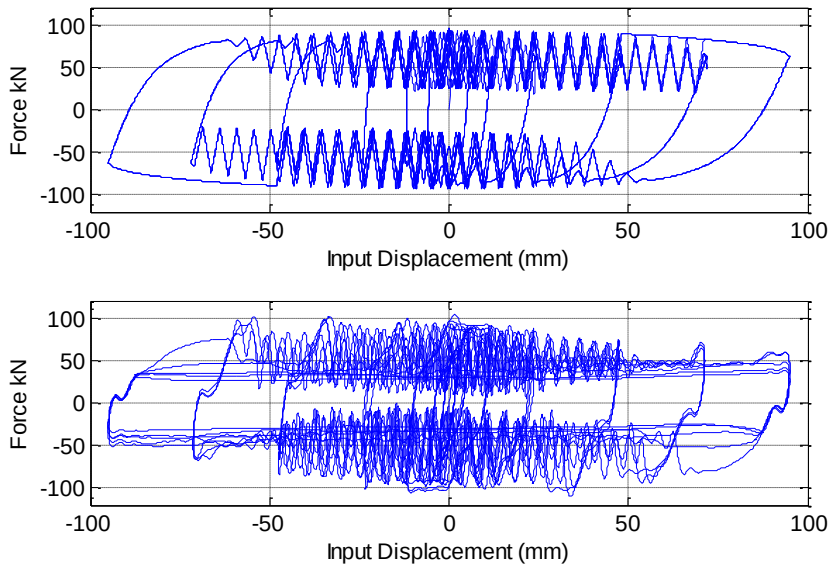

Figure 9: Comparison between exponential model and filtered data when using the added dynamics from Equation (5).

Model 3: Rounded Menegotto-Pinto with Random Stick Slip Behaviour

Finally, if greater accuracy is desired, to capture the rounded corners in Figure 4 as device input switches direction, a threshold term may be defined using an exponential. The model of Equations (3)-(4) may thus be extended:

$$F_1 = 2F_{static}\,(1 - \exp\frac{x}{A(amp)}) \qquad (6)$$

Overall, Equations (3)-(6) are general and will capture a range of experimentally observed behaviour, be it stick-slip induced or a result of different mechanisms. The resulting terms can be implemented in any non-linear analysis code that manages similar hysteretic models to the MP model. For validation the model is compared to experimental results qualitatively to avoid over-modelling of noise or device specific effects. Results are shown for each term in Equations (3)-(6) to delineate the effects captured.

RESULTS AND DISCUSSION

Figure 8 shows results for the bilinear Menegotto-Pinto curve with stick slip using Equation (3), Equation (4), and constant amplitude. The model parameter values are given in Table 1 to show the model can be generalized to any similar situation, including one without oscillations. It is clear that it captures the fundamental dynamics observed.

Table 1: Basic model parameters for Figure 8

Parameter	Value
K (kN/mm)	32
F_{static} *(kN)*	62
$F_{kinetic}$ *(kN)*	25
β and γ	100
Number of peaks	93

Figure 9 shows results for Model 2 with the bilinear Menegotto-Pinto and random stick slip behaviour defined in Equation (5). Table 2 shows the model parameters, which are unchanged from Table 1, except for the extra values added when using this added model term. The results further reinforce the general nature of this model. Comparison to the experimental data of Figures 4 and 9 (bottom) shows a much better match.

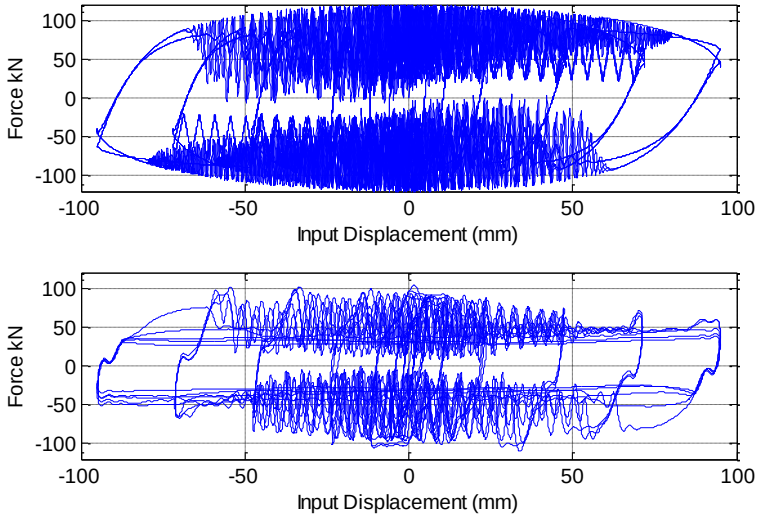

Figure 10: Comparison between model 3, using all of Equations (3)-(6) (top) and filtered experimental data (bottom).

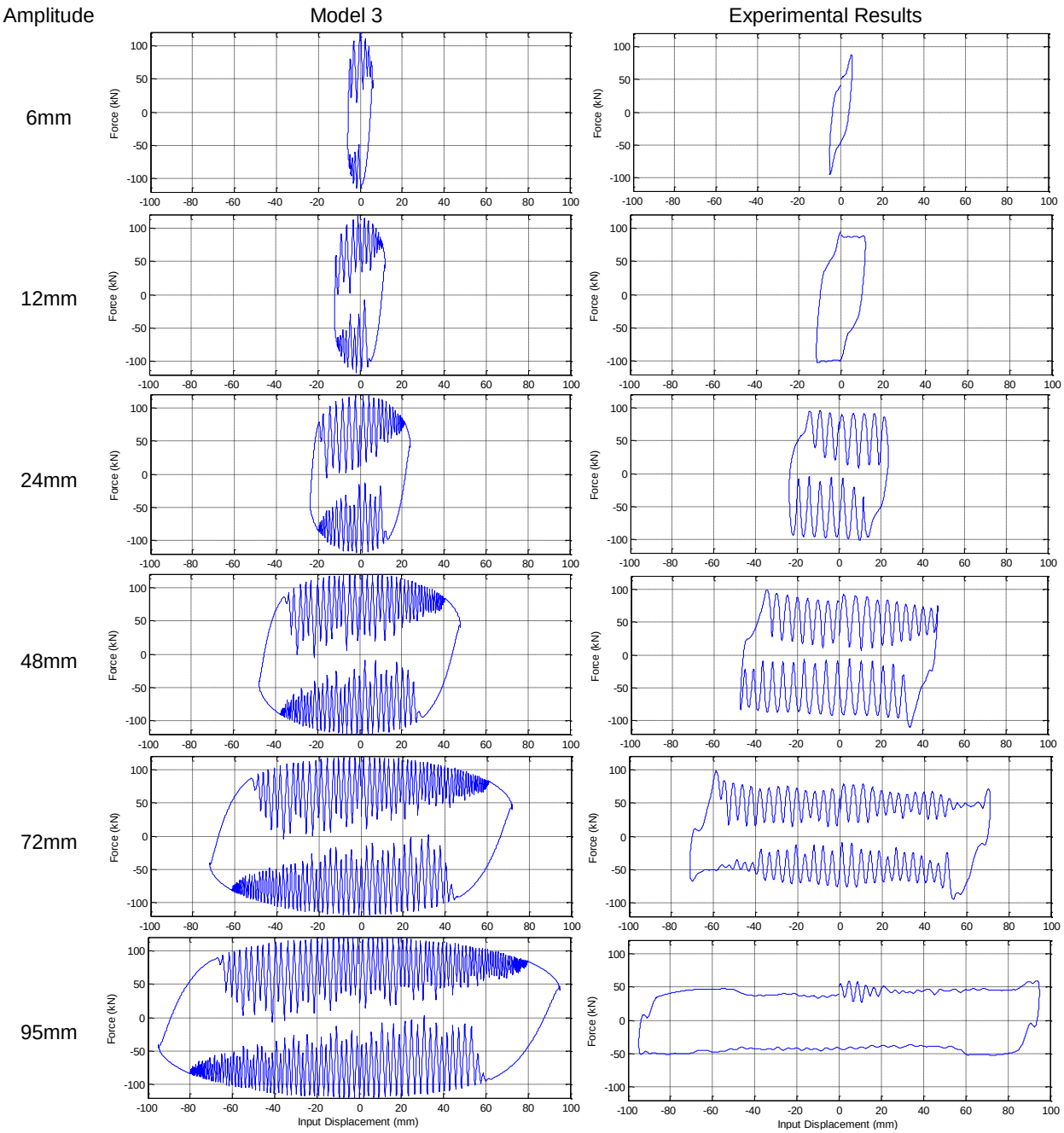

Figure 11: Comparison between model and experimental data for the 3rd cycle at each amplitude

Table 2: Second model parameters

Parameter	Value
K (kN/mm)	32
F_{static} *(kN)*	62
$F_{kinetic}$ *(kN)*	25
β and γ	100
Number of peaks	61
A(amp)	$0.1x_{max}+1$

Figure 10 shows behaviour for Model 3 with the rounded Menegotto-Pinto and random stick slip behaviour using Equation (5) and Equation (6) included to capture the change in amplitude over displacement in a direction. This behaviour improves the match to experimental results. The apparent difference in effective ‘’period’’ of oscillations over displacement is due to the repeated size of these oscillations as defined by the model.

It should be noted that the remaining differences like the random dynamics added, are due to observed, but unknown nonlinearities in the device experiments. Additional modelling to capture them risks over-modelling, where the results of all cases may well be adequate. Importantly, the results and methods presented can be generalized to similar systems. Thus, if further research quantifies certain effects due to specific shim materials or other factors, they can be readily incorporated into this model by a similar basic extension if required.

Finally, Figure 11 shows the 3rd cycle from each of the six increasing input amplitudes of Figure 4b for the experiment and from the model in Figure 10 for better comparison. The main difference between experimental data and model is the inflection point at the beginning of each cycle. This inflection point is attributed to ‘pinching’ of the SHJ and bolt movement during load reversal. The phenomenon is not modelled within this study and is device and clamping force specific.

Overall, this research provides a means by which irregular device behaviour can be modelled and incorporated into larger structural-level time-history analysis. The general influence of the specific energy dissipation device mechanics on the overall response of the structure can then be assessed and provide important insight for designers. In many cases, a more irregular, stick-slip mechanism of a friction connection may not adversely affect the overall structure performance, but this influence should be carefully considered.

CONCLUSIONS

A model to capture the observed irregularities of experimental data for a specific sliding friction connection has been developed from a basic Menegotto-Pinto hysteresis model. This base model reproduced the underlying cyclic elasto-plastic behaviour. The MP model was then modified to incorporate stick-slip phenomena observed for some friction materials in these devices in a general fashion that allows any similar, irregular experimental observations to be equally captured. Further, model modifications can include specifics such as random oscillations within an observed range and the more natural rounded elasto-plastic curve, all of which can be tailored to match an observed device or system behaviour. The results and modelled elements are validated against observed experimental data with good qualitative matching. The generality of the model ensures such behaviours can be captured to better assess in computational design procedures any likely loss of force and dissipation for structures using these devices. Overall, a detailed model is presented that captures the important aspects of the nonlinear dynamic SHJ response observed. It also provides new insight into the response mechanisms, accurately models the stick-slip mechanism of the friction interface, and can be generalized to a wide range of similar systems or devices.

ACKNOWLEDGEMENTS

The authors gratefully acknowledge funding from the MBIE Natural Hazards Research Platform.

REFERENCES

Clifton, C., “Semi-Rigid Joints for Moment-Resisting Steel Framed Seismic-Resisting Systems”, *PhD Thesis in Civil Engineering*. University of Auckland, 2005 .

Khoo, H.H., C. Clifton, J. Butterworth, G. MacRae, S. Gledhill, and G. Sidwell, “Development of the self-centering Sliding Hinge Joint with friction ring springs”. *Journal of Constructional Steel Research*, (2012a). 78: p. 201-211.

Khoo, H.H., G.C. Clifton, J.W. Butterworth, and G.A. MacRae, “Shim and bolt size effects on the Asymmetric Friction Connection”. *STESSA 2012: Proceedings of the 7th International Conference on Behaviour of Steel Structures in Seismic Areas*, (2012b).

Khoo, H.H., C. Clifton, J. Butterworth, G. MacRae, and G. Ferguson, “Influence of steel shim hardness on the Sliding Hinge Joint performance”. *Journal of Constructional Steel Research*, (2012c) 72: p. 119-129.

MacRae, G.A., C. Clifton, N. MacKinven, J. Mago, J. Butterworth, and S. Pampanin, “The Sliding Hinge Joint Moment Connection”. *Bulletin of the New Zealand Society for Earthquake Engineering*, 2010. 43(3): p. 202-212.

Menegotto, M. and P. Pinto, “Method of analysis for cyclically loaded reinforced concrete plane frames including changes in geometry and non-elastic behavior of elements under combined normal force and bending”, *in Proc. Symp. Resistance and Ultimate Deformability of Struct. Acted on by Well-Defined Repeated Loads*, IABSE Reports, Volume 13. 1973, IABSE Reports: Lisbon, Portugal.

Sivaselvan, M.V. and A.M. Reinhorn, “Hysteretic models for deteriorating inelastic structures”. *Journal of Engineering Mechanics-ASCE*, 2000. 126(6): p. 633-640.